Supporting Information for:

In situ fabrication of $BiOBr_xCl_{1-x}$ photocatalysts with regulated electronic structure and enhanced visible light photocatalytic performance

Haoyu Zhang[a], Xia Zhang[a], Liman Peng[c], Jiaxin Liu[a], Yiguo Su[b*] and Shushu Huang[a*]

[a]*College of Light Industry and Textile, Inner Mongolia University of Technology, Hohhot, 010080, China*

[b]*Inner Mongolia Key Laboratory of Chemistry and Physics of Rare Earth Materials, College of Chemistry and Chemical Engineering, Inner Mongolia University, Hohhot, 010021, China*

[c]*Transportation Institute, Inner Mongolia University, Hohhot, Inner Mongolia 010021, China*

1. Experimental section

1.1 Catalysts preparation

$BiOBr_xCl_{1-x}$ (x=0, 0.25, 0.5 0.75, 1) samples were produced via the simple hydrothermal method. Briefly, 0.5 mmol of $Bi(NO_3)_3 \cdot 5H_2O$ was dissolved into 10 mL ethylene glycol to get solution A. And 0.5 mmol NaX containing different molar ratio of NaCl and NaBr was added into 10 mL deionized water to get solution B. Then A was injected to solution B with stirred vigorously and a suspension was obtained. Finally, the mixture was transferred into a 25 mL Teflon-lined autoclave and heated at 180 ^oC for 6h. The resultant precipitates were washed with deionized water consecutively and dried 12h at 60 ^oC. The final products were named as BiOCl,

$BiOBr_{0.25}Cl_{0.75}$, $BiOBr_{0.5}Cl_{0.5}$, $BiOBr_{0.75}Cl_{0.25}$ and BiOBr.

1.2 Sample characterization

The wide-angle X-ray power diffraction (XRD) performing on a Rigaku DMAX2500 X-ray diffractometer with Cu Kα radiation was carried out in order to investigate the crystal phase structures. Transmission electron microscopy (TEM) was performed on a FEI Tecnai G2 F20 S-TWIN field emission microscope apparatus with an acceleration voltage of 200 kV, which applied to investigate the morphologies of the obtained photocatalysts. Perkin Elmer UV/VS/NIR Lambda 750 s spectrometer was performed to measure the ultraviolet-visible DRS of the obtained products. X-ray Photoelectron Spectroscopy (XPS) analyses were performed on an ESCALab220i-XL with a monochromatic Al Kα and charge neutralizer. The C 1s peak at 284.6 eV was used for the referenced binding energy for samples. The specific surface areas of samples were measured by a Micromeritics ASAP 2020 Surface Area and Porosity Analyzer by Brunauer-Emmett-Teller (BET) technique. The photoluminescence (PL) and time-resolved fluorescence decay spectra were measured on an Edinburgh Instruments FLS920 spectrofluorimeter equipped with both continuous and pulsed xenon lamps. And the excitation wavelength for photoluminescence analysis was 315 nm. The transient photocurrent response of the samples with light on/off cycles were carried out on the Metrohm Autolab (PGST AT302N) under white (neutral) light irradiation (LED 690 lm, $[Na_2SO_4]$ = 0.2 M) biased at 0.5 V vs. Ag/AgCl (saturated KCl). Electrochemical impedance spectroscopy (EIS) measurements were performed to investigate the migration rate of charge carrier with the frequency from 0.1 Hz to

100 KHz. Na_2SO_4 aqueous solution (0.2 M, pH = 7) was served as the electrolyte. Electron paramagnetic resonance (EPR) spectra for $\cdot O_2^-$ and ·OH were determined in dark and under visible light irradiation (methanol solution volume, 2.0 mL; sample, 4 mg; DMPO, 0.22M).

1.3 Photocatalytic performance measurement

The photocatalytic performance of photocatalyst was evaluated by the photocatalytic Rhodamine B (RhB) degradation under visible light irradiation. In brief, 15 mg samples were dispersed in 30 mL RhB solution (20 mg/L) with magnetic stirring. Before irradiation, the suspension was treated in dark for 60 min to achieve the adsorption-desorption equilibrium. Then, the suspensions were irradiated under 300 W xenon lamp with a filter ($\lambda \geq 420$ nm). 4 mL of suspension was collected at the interval of 30 min and centrifuged during the reaction process, which was analyzed by UV-vis spectrophotometer.

Fig. S1 Enlarged XRD patterns of the prepared samples.

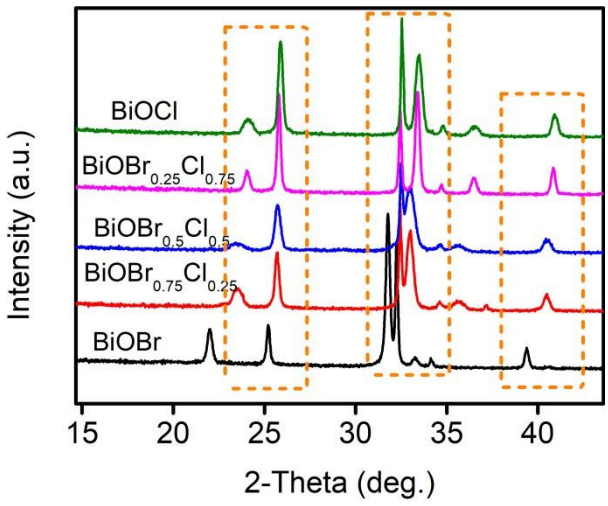

Fig. S2 SEM images of the prepared $BiOCl_{1-x}Br_x$ samples (x=0 (a); x=1 (b); x=0.25 (c, d); x=0.5 (e); x=0.75 (f)).

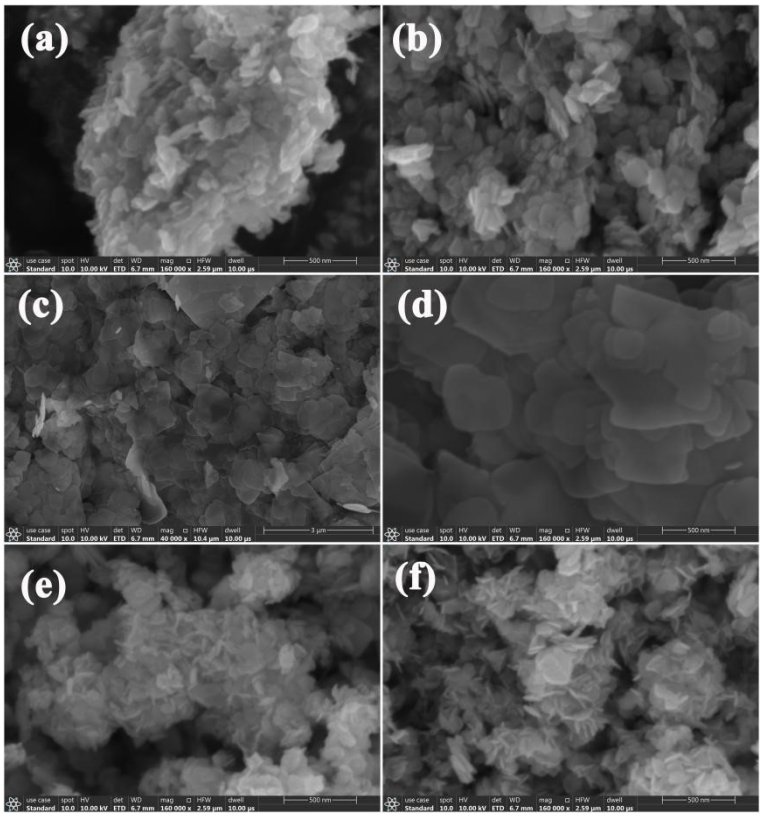

Fig. S3 TEM images of BiOCl and BiOBr.

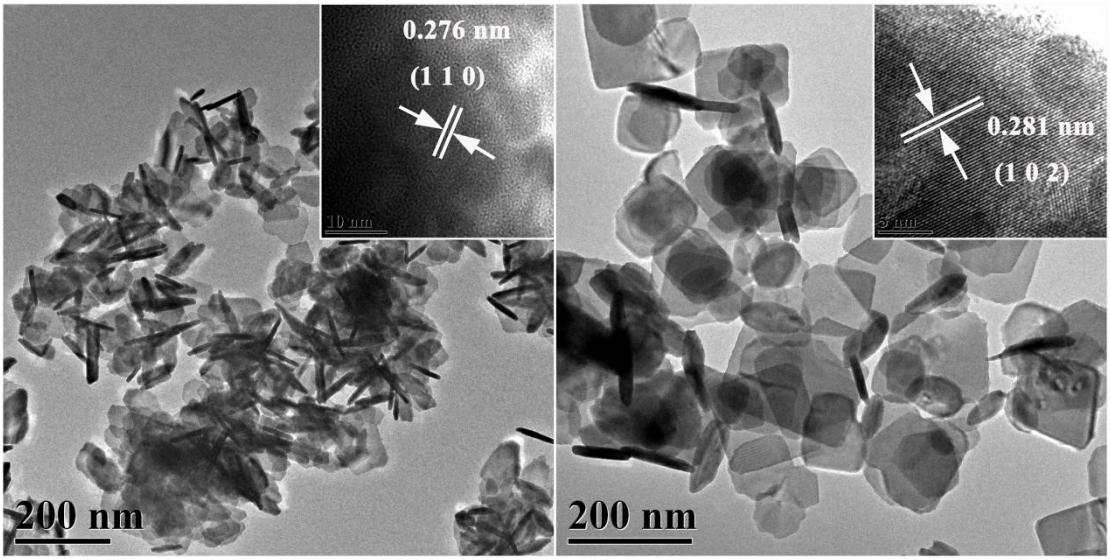

Fig. S4 UV-visible diffuse reflectance spectra of the prepared samples.

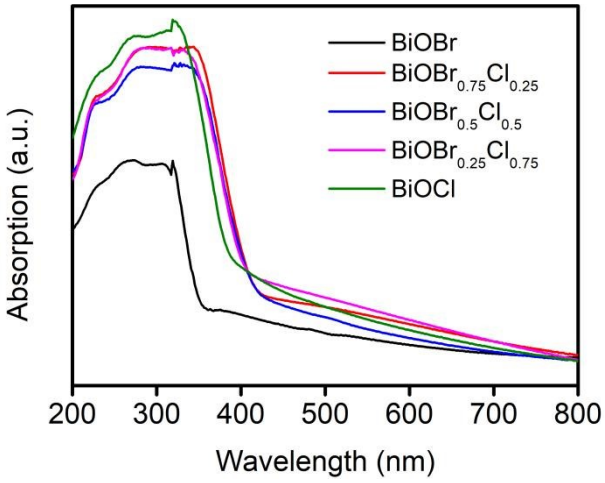

Fig. S5 Electronic structures of BiOCl, BiOBr and $BiOBr_{0.25}Cl_{0.75}$ samples.

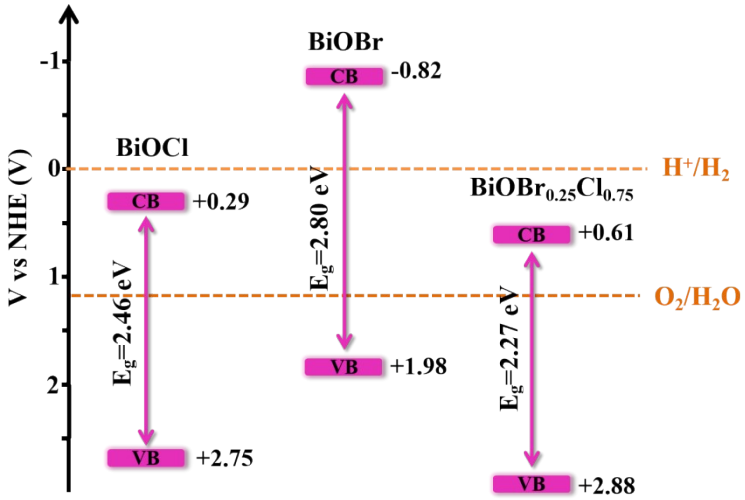

Fig. S6 Valence band X-ray photoelectron spectroscopy (VB-XPS) analysis of BiOCl, BiOBr and $BiOBr_{0.25}Cl_{0.75}$ samples.

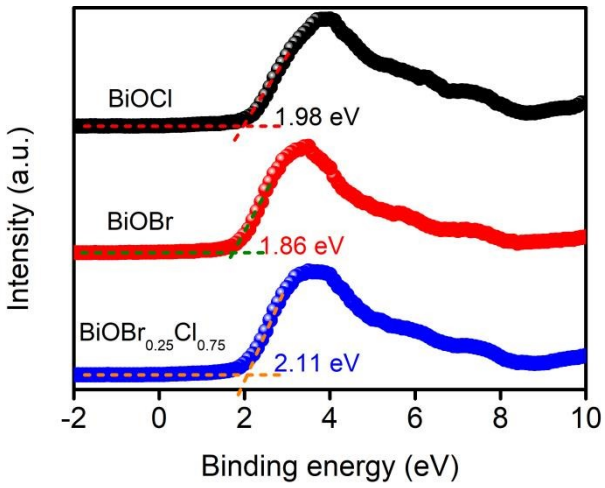

Fig. S7 XPS survey spectra of BiOCl, BiOBr and $BiOBr_{0.25}Cl_{0.75}$ samples.

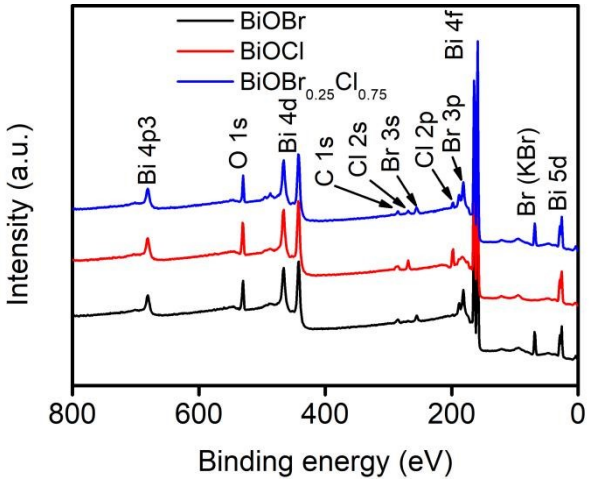

Fig. S8 The relationship between ln (C_0/C) and irradiation time for the degradation of RhB over all samples.

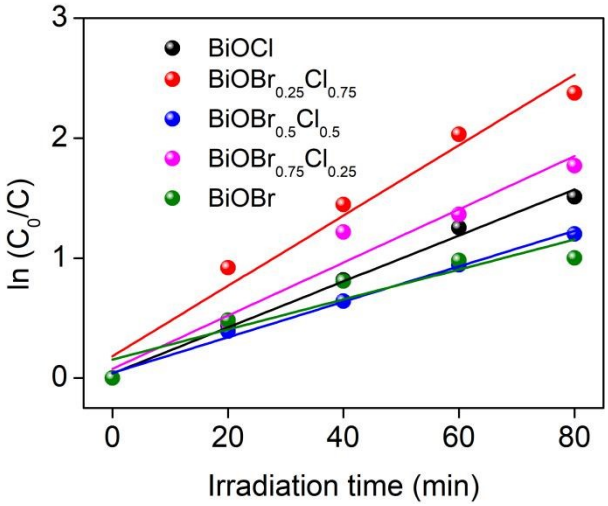

Fig. S9 Removal efficiency of RhB by $BiOBr_{0.25}Cl_{0.75}$ sample in real water body.

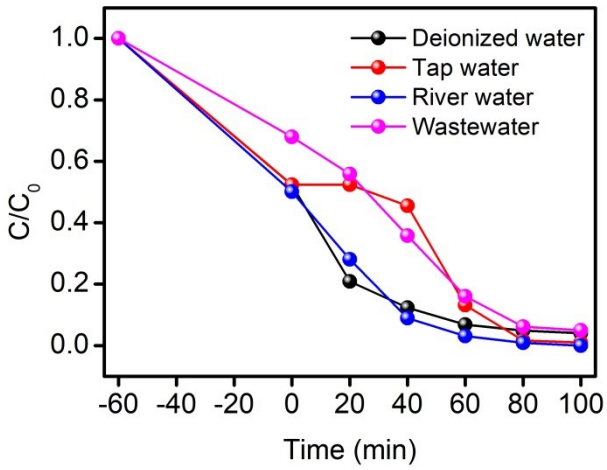

Table S1 Comparison of catalytic performance of $BiOBr_{0.25}Cl_{0.75}$ with that of other catalysts reported in the literature.

Entry	Sample	Light source	Removal efficiency (%)	Ref.
1	$BiOBr_{0.25}Cl_{0.75}$	300 W Xe lamp ($\lambda \geq 420$ nm)	96.0	This work
2	20-BiOCl	450 W Xe lamp ($\lambda > 400$ nm)	99.9	1
3	$Ag/BiOCl/AgIO_3$	500 W Xe lamp	91.0	2
4	$BiOCl/CeO_2$	245 W Xe lamp	98.8	3
5	Bi/BPNs/P-BiOCl	300 W Xe lamp	99.0	4
6	Bi/BiOCl-1	500 W Xe lamp	98.0	5
7	Br-BOCl-1	500 W Xe lamp ($\lambda > 420$ nm)	90.0	6
8	BiOBr-acid-0.5	300 W Xe lamp ($\lambda > 420$ nm)	96.0	7
9	BCA20	210 W Xe lamp ($\lambda \geq 420$ nm)	91.8	8
10	$P_{0.15}BiO_x$	400 W Hg lamp ($\lambda \geq 400$ nm)	96.0	9
11	$Bi/BiOBr_{0.5}Cl_{0.5}$-0.3	300 W Xe lamp ($\lambda \geq 400$ nm)	85.0	10

12	BiOCl-NaCl	300 W Xe lamp ($\lambda \geq 400$ nm)	92.7	11
13	BiOBr@TiO_2-6 NFM	300 W Xe lamp ($\lambda \geq 420$ nm)	95.5	12
14	BiOBr/$Bi_{24}O_{31}Br_{10}$	500 W Xe lamp ($\lambda > 420$ nm)	92.4	13
15	BiOCl/CAU-17	300 W Xe lamp ($\lambda \geq 420$ nm)	96.3	14

Fig. S10 Recycling experiment for photocatalytic RhB degradation over $BiOBr_{0.25}Cl_{0.75}$ sample.

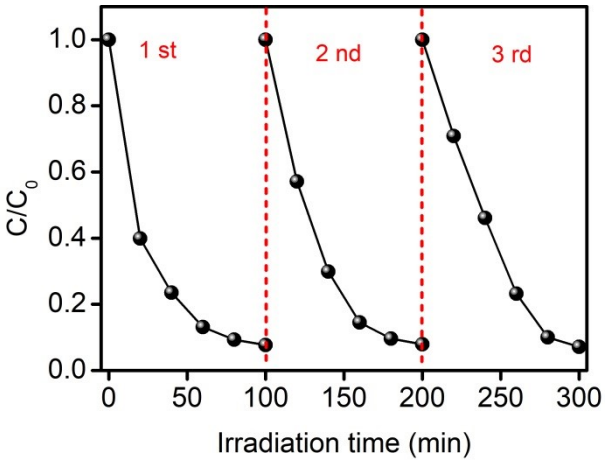

Fig. S11 Photocatalytic tetracycline (TC) degradation efficiency over the prepared samples.

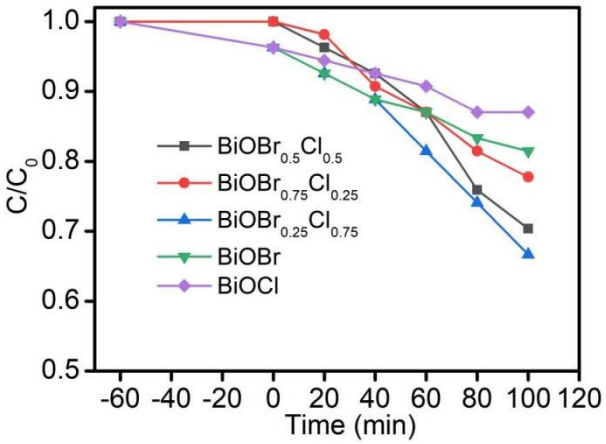

Fig. S12 Photoluminescence (PL) spectra of BiOCl, BiOBr and $BiOBr_{0.25}Cl_{0.75}$ samples.

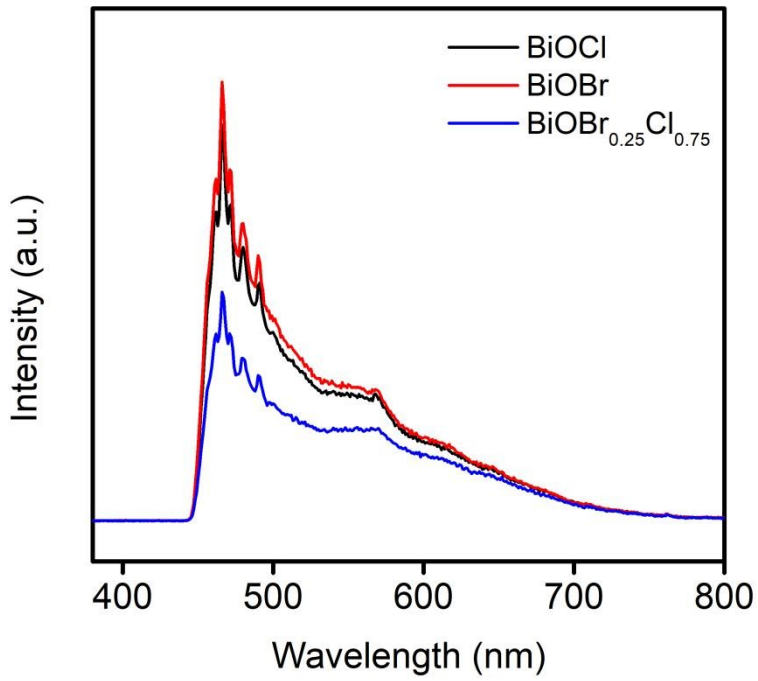

Fig. S13 Electrochemical impedance spectroscopy (EIS) Nyquist plots of BiOCl, BiOBr and $BiOBr_{0.25}Cl_{0.75}$ samples.

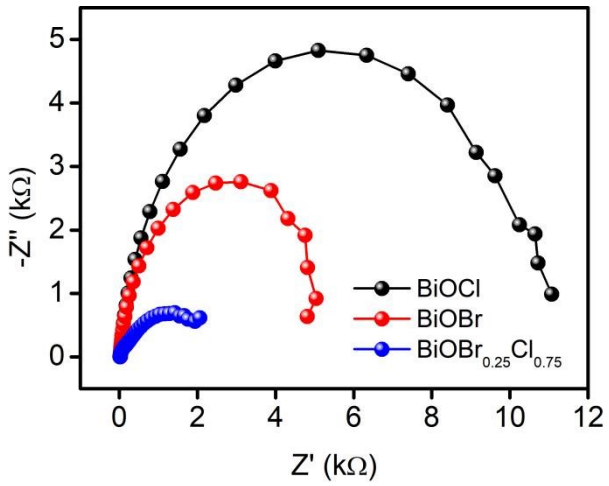

References:

1. K. E. Ahmed, D. H. Kuo and L. W. Duresa, *J. Ind. Eng. Chem.*, 2020, **83**, 200-207.
2. D. Zhang, G. Tan, M. Wang, B. Li, M. Dang, Y. Wang, B. Zhang, H. Ren and A. Xia, *Appl. Surf. Sci.*, 2020, **530**, 147228.
3. Y. Zhang, Q. Shao, H. Jiang, L. Liu, M. Wu, J. Lin, J. Zhang, S. Wu, M. Dong and Z. Guo, *Inorg. Chem. Front.*, 2020, **7**, 1345-1361.
4. H. Ma, Y. Wang, Z. Zhang, J. Liu, Y. Yu, S. Zuo and B. Li, *Chemosphere*, 2023, **330**, 138717.
5. Y. Yu, Z. Yang, Z. Shang and X. Wang, *J. Phys. Chem. Solids*, 2023, **174**, 111172.
6. Q. Zhang, W. Nie, T. Hou, H. Shen, Q. Li, C. Guan, L. Duan and X. Zhao, *Nanomaterials*, 2022, **12**, 2423.
7. Z. Wang, Z. Chu, C. Dong, Z. Wang, S. Yao, H. Gao, Z. Liu, Y. Liu, B. Yang and H. Zhang, *ACS Appl. Nano Mater.*, 2020, **3**, 1981-1991.
8. X. Zheng, W. Chen, M. Xu, C. Cai and F. Yang, *J. Nanopart. Res.*, 2023, **25**, 96.
9. Z. Khazaee, A. R. Mahjoub, A. H. C. Khavar, V. Srivastava and M. Sillanpää, *Sol. Energy*, 2020, **207**, 1282-1299.
10. T. Dong, G. Jiang, Y. He, L. Yang, G. Wang and Y. Li, *J. Hazard. Mater.*, 2022, **428**, 128207.
11. W. Dong, T. Xie, Z. Wu, H. Peng, H. Ren, F. Meng and H. Lin, *RSC Adv.*,

2021, **11**, 38894-38906.

12. Y. Cai, J. Song, X. Liu, X. Yin, X. Li, J. Yu and B. Ding, *Environ. Sci.: Nano*, 2018, **5**, 2631-2640.

13. G. Huang, Z. Li, K. Liu, X. Tang, J. Huang and G. Zhang, *Catal. Sci. Technol.*, 2020, **10**, 4645-4654.

14. F. Zhang, X. Xiao and Y. Xiao, *Dalton T.*, 2022, **51**, 10992-11004.